Modeling the Fitness Consequences of a Cyanophage-Encoded Photosynthesis Gene

Citation: Bragg JG, Chisholm SW (2008) Modeling the Fitness Consequences of a Cyanophage-Encoded Photosynthesis Gene. PLoS ONE 3(10): e3550. doi:10.1371/journal.pone.0003550

As Published: http://dx.doi.org/10.1371/journal.pone.0003550

Publisher: Public Library of Science

Persistent URL: http://hdl.handle.net/1721.1/55289

Version: Final published version: final published article, as it appeared in a journal, conference proceedings, or other formally published context

OPEN ACCESS Freely available online

PLoS one

Modeling the Fitness Consequences of a Cyanophage-Encoded Photosynthesis Gene

Jason G. Bragg[1]*, **Sallie W. Chisholm**[1,2]

1 Department of Civil and Environmental Engineering, Massachusetts Institute of Technology, Cambridge, Massachusetts, United States of America, **2** Department of Biology, Massachusetts Institute of Technology, Cambridge, Massachusetts, United States of America

Abstract

Background: Phages infecting marine picocyanobacteria often carry a *psbA* gene, which encodes a homolog to the photosynthetic reaction center protein, D1. Host encoded D1 decays during phage infection in the light. Phage encoded D1 may help to maintain photosynthesis during the lytic cycle, which in turn could bolster the production of deoxynucleoside triphosphates (dNTPs) for phage genome replication.

Methodology / Principal Findings: To explore the consequences to a phage of encoding and expressing *psbA*, we derive a simple model of infection for a cyanophage/host pair — cyanophage P-SSP7 and *Prochlorococcus* MED4— for which pertinent laboratory data are available. We first use the model to describe phage genome replication and the kinetics of *psbA* expression by host and phage. We then examine the contribution of phage *psbA* expression to phage genome replication under constant low irradiance (25 μE m^{-2} s^{-1}). We predict that while phage *psbA* expression could lead to an increase in the number of phage genomes produced during a lytic cycle of between 2.5 and 4.5% (depending on parameter values), this advantage can be nearly negated by the cost of *psbA* in elongating the phage genome. Under higher irradiance conditions that promote D1 degradation, however, phage *psbA* confers a greater advantage to phage genome replication.

Conclusions / Significance: These analyses illustrate how *psbA* may benefit phage in the dynamic ocean surface mixed layer.

Citation: Bragg JG, Chisholm SW (2008) Modeling the Fitness Consequences of a Cyanophage-Encoded Photosynthesis Gene. PLoS ONE 3(10): e3550. doi:10.1371/journal.pone.0003550

Editor: Andrew David Millard, University of Warwick, United Kingdom

Received May 22, 2008; **Accepted** October 3, 2008; **Published** October 29, 2008

Funding: This work was supported in part by funds from the US National Science Foundation, the Gordon and Betty Moore Foundation Marine Microbiology Initiative, and the US Department of Energy GTL Program. It is an NSF C-MORE contribution.

Competing Interests: The authors have declared that no competing interests exist.

* E-mail: jbragg@mit.edu

Introduction

The marine picocyanobacteria *Prochlorococcus* and *Synechococcus* are numerically dominant phytoplankton in nutrient-poor open ocean ecosystems, and are an important contributor to photosynthesis in the oceans [1–3]. They are infected by cyanophages including members of the families Podoviridae, Myoviridae and Siphoviridae [4], which can be abundant in regions where these cells dominate (*e.g.* [5–8]). Several genomes of these marine cyanophages have been sequenced, revealing gene content and organization broadly similar to confamilial phages [9–11]. For example, cyanophage P-SSP7, which infects *Prochlorococcus* MED4, has many genomic similarities to the T7 phage that infects *Escherichia coli* [11].

The genomes of marine *Synechococcus* and *Prochlorococcus* cyanophages often contain genes that are absent from the genomes of morphologically related phages that do not infect marine cyanobacteria [11]. A striking example of this is the *psbA* photosynthesis gene [12,13]. This gene is found in the genomes of a large proportion of cyanophages known to infect marine picocyanobacteria [14,15], suggesting that it confers a fitness advantage. The product of the *psbA* gene in the host cell, the D1 protein, forms part of the photosystem II reaction center, and turns over relatively rapidly during photosynthesis [16]. Over the course of phage infection, host-encoded D1 proteins decline following the inhibition of host transcription and the decay of host *psbA* transcripts [17], while phage-encoded D1 proteins increase [17]. It is hypothesized that the latter replace damaged host D1 proteins, and help to maintain photosynthesis throughout the lytic cycle. This, in turn, could increase the relative fitness of phage that carry the *psbA* gene [12,18]. In some cyanophages, reproduction (*e.g.* [19]) and genome replication [17] are severely limited in the dark, indicating that photosynthesis can be important for phage genome replication, which potentially limits the production of phage progeny. During the cyanophage P-SSP7 lytic cycle, *psbA* is transcribed contemporaneously with several metabolism genes that have probable roles in dNTP synthesis (*e.g.* ribonucleotide reductase), as well as genome replication enzymes [20]. This adds weight to the suggestion that the *psbA* gene helps phage P-SSP7 to acquire resources to make dNTPs during infection.

Models of phage infection in well established phage/host systems, such as T7/*E. coli* [21], have provided significant insights into factors affecting phage reproduction and fitness [22–24]. Inspired by these works, we have developed an intracellular model of infection of *Prochlorococcus* MED4 by the Podovirus P-SSP7. The model concentrates on processes of phage genome replication, the

production of dNTPs, and the expression of *psbA* by host and phage, and can find good agreement with experimental measurements collected over the cyanophage P-SSP7 lytic cycle [17,20]. We use the model to ask basic questions about the advantages to the phage of carrying this gene that are not yet tractable experimentally: How much can phage *psbA* expression benefit phage genome replication? To what degree is this contingent on environmental conditions, particularly the ambient light environment?

Methods

Model Development

(a) Approach. After the genome of cyanophage P-SSP7 enters a host cell, phage genes are expressed, the phage genome is replicated, new phage particles are assembled, and the host cell is lysed — all over a period of about 8 hours [20]. Many of these processes are carried out using products of phage-encoded genes, which are expressed at different times during the cycle of infection [20]. Our model links phage genome replication to the production of deoxynucleoside triphosphates (dNTPs), which in turn is linked to photosynthesis and the kinetics of host and phage *psbA* expression (Fig. 1). It incorporates elements of previous models of phage genome replication [21,25], and D1 protein kinetics [26]. More specifically, we model phage genome replication within a host cell as a function of the availability of dNTPs, which are supplied by (i) scavenging from the degraded host genome, and (ii) a pathway for the synthesis of new deoxynucleotides. We assume that the supply of dNTPs from each of these sources can depend on photosynthesis. In turn, photosynthesis is modeled as a function of the number of functional photosystem II (PSII) subunits, which become non-functional when their D1 core proteins are damaged, and regain their function when the damaged D1 is excised from the photosystem and replaced with the protein product of either a host or phage *psbA* gene (Fig. 1).

Our model incorporates processes that are carried out by phage genes that begin to be expressed at different times following infection [20]. We therefore need a way to represent relatively abrupt increases in the velocity of processes that are carried out by different proteins (generically, P), at different, specific times following infection. We do this using Hill functions [27], or $P_x = \frac{t^n}{t^n + t_x^n}$, where t is the time since infection, t_x is the time at which process P_x reaches half its maximum rate (the 'timing parameter'), and n is a parameter that controls the abruptness of the increase. The Hill function is a sigmoidal curve that increases from zero to one with increasing values of t, and can provide a reasonable description of the expression of some relevant phage genes, at least in terms of mRNA abundances (see Text S1). Below, we represent Hill functions in our equations using 'P' followed by a subscript that corresponds to the process that is being represented.

(b) Phage genome replication. We assume that protein products of phage genes, such as DNA polymerase, are essential for phage genome replication. Following the expression of these genes, genome replication occurs as a function of the availability of dNTPs, N (Fig. 1). We model the change in phage genomes in a host cell (G_P) over time (following [21,25]), as

$$\frac{d(G_P)}{dt} = \frac{1}{L_P}\frac{V_r N}{N + K_{mr}} P_r. \quad (1)$$

Here L_P is the length of the phage genome (in base pairs). The term P_r is a Hill function that represents the time-dependent expression of phage genome replication genes. V_r represents the maximum rate of DNA elongation per functional unit of phage genome replication machinery (hereafter, polymerase), multiplied by the maximum abundance of polymerases. K_{mr} is the value of N at which elongation by a polymerase reaches half its maximum rate. We set $G_P(0) = 1$, to reflect infection by a single virion.

(c) Phage acquisition of dNTPs. We assume that cyanophage P-SSP7 can acquire dNTPs from two possible sources during infection of *Prochlorococcus* MED4 (Fig. 1). The first is scavenging from the host genome, which is degraded during infection [20]. The second involves the synthesis of new deoxynucleotides [11].

We model degradation of the host's genome (G_H) as

$$\frac{d(G_H)}{dt} = -\frac{V_{Gdeg} G_H}{G_H + K_{mGH}} P_{Gdeg}, \quad (2)$$

where P_{Gdeg} is a Hill function representing the expression of genes that degrade the host genome (with time parameter t_{Gdeg}), and V_{Gdeg} is the maximum rate of degradation of the host genome. The term $\frac{V_{Gdeg} G_H}{G_H + K_{mGH}}$, with small K_{mGH}, is approximately equal to V_{Gdeg} until the host genome is almost entirely degraded. This formulation is based on the observation that the decline in host genomes is approximately linear, following a delay of 4–5 h [20], as well as the necessity for degradation to cease as G_H approaches 0. We set $G_H(0) = 1$ to reflect a single host genome at the time of infection.

We assume the phage can then make dNTPs from the degraded host genome (G_{Hdeg}). We model the rate of production of dNTPs from this source (s_G; dNTPs cell^{-1} h^{-1}) as $s_G = 2L_H \frac{V_N G_{Hdeg}}{G_{Hdeg} + K_N} P_{Gdeg}$. Here $2L_H$ is the number of deoxynucleotides in the host genome (2 per base pair, times L_H base pairs per genome), and V_N is the maximum rate at which the degraded genome can be converted to dNTPs. We set the parameter K_N to a small value so that when genes for degrading the host genome are expressed and degraded host genome is available, the term $\frac{G_{Hdeg}}{G_{Hdeg} + K_N} P_{Gdeg}$ is approximately equal to 1, and dNTPs are produced from degraded genomes at a rate of approximately $2L_H V_N$.

We then consider the possibility that the production of dNTPs from degraded genomes ($2L_H V_N$) is limited by photosynthesis. We represent this in the model by letting $2L_H V_N = \varepsilon + \mu$, where ε represents the rate at which dNTPs can be made from degraded genomes during infection in the dark, and μ represents the photosynthesis-dependent production of dNTPs from host genomes. In turn, we assume that μ is limited by the abundance of functional photosystem II subunits or $\mu = z\gamma F_{PSII}$, where F_{PSII} is the number of functional photosystem II subunits per cell, γ is the rate of photosynthesis per functional PSII, and z is the efficiency with which products of photosynthesis are used in converting degraded genomes to dNTPs. Below, we develop a model for the proportion of PSII subunits that are functional (f_{PSII}) during infection. We therefore let $F_{PSII} = Uf_{PSII}$, where U is the total number of PSII subunits per cell. This means we have $\mu = z\gamma U f_{PSII}$, or if we represent $z\gamma U$ by the parameter κ (in dNTPs cell^{-1} h^{-1}), $\mu = \kappa f_{PSII}$.

We note that the change over time in the proportion of the host genome in a degraded state is then given by

$$\frac{d(G_{Hdeg})}{dt} = \frac{V_{Gdeg} G_H}{G_H + K_{mGH}} P_{Gdeg} - \frac{V_N G_{Hdeg}}{G_{Hdeg} + K_N} P_{Gdeg}. \quad (3)$$

We now consider the possibility that new deoxynucleotides (*i.e.*, not from the host genome) are produced during infection as a source of dNTPs for phage genome replication (s_P; dNTPs cell^{-1} h^{-1}). This possibility is suggested by the observation that cyanophage P-SSP7 encodes [11] and transcribes [20] a ribonucleotide reductase gene, whose protein product likely

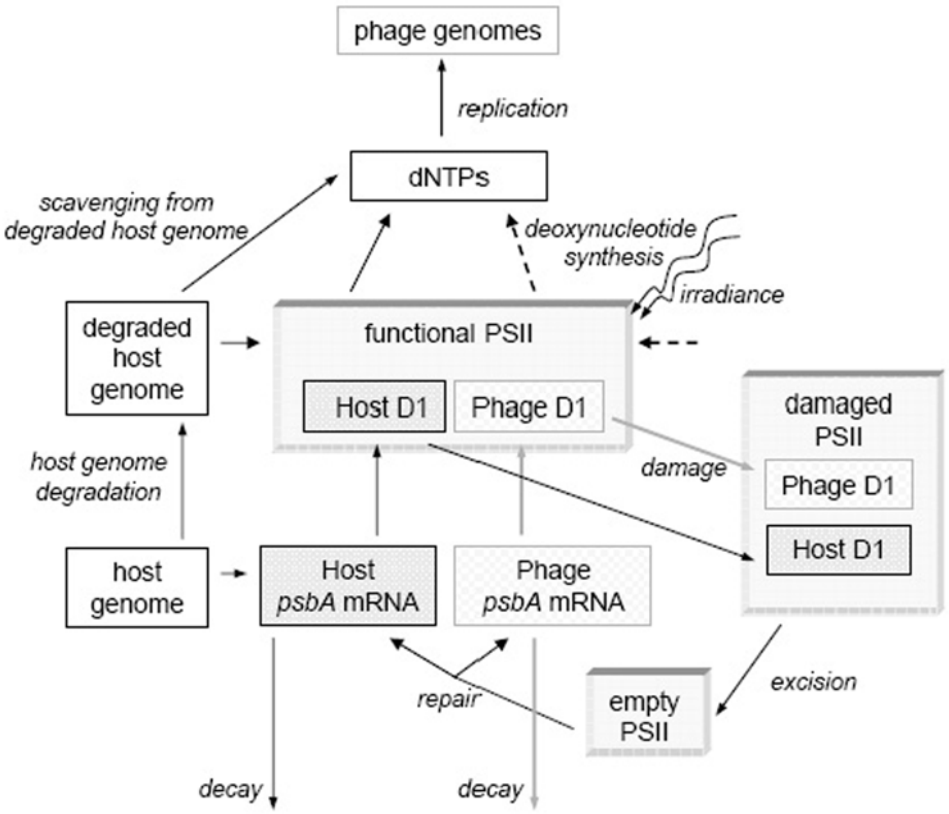

Figure 1. Schematic diagram of model. Phage genomes are made using dNTPs from two possible sources. First, dNTPs can be made by scavenging deoxynucleotides from the host genome. This process can occur in the dark, but is bolstered by photosynthesis. Second, dNTPs can be newly synthesized by a process that is dependent on the products of photosynthesis (dashed lines). Photosynthesis is dependent on functional PSII subunits, which contain the D1 protein. During exposure to light, D1 proteins can become damaged, and are excised from PSII subunits, and replaced with D1 proteins from either host or phage encoded *psbA* mRNAs.
doi:10.1371/journal.pone.0003550.g001

functions in converting ribonucleotides to deoxynucleotides. We assume this source of dNTPs is dependent on photosynthesis, as well as the activity of genes that are encoded by the phage, and whose expression is described by a Hill function, P_S. Once these phage genes are expressed, the rate of supply of dNTPs from this source is assumed to be proportional to the rate of photosynthesis, which is limited by the abundance of functional PSII subunits, or $s_P = v\gamma F_{PSII} P_S$, where v is the efficiency with which products of photosynthesis are converted to dNTPs. We then represent $v\gamma U$ using a single parameter, λ (in dNTPs cell^{-1} h^{-1}), such that $s_P = \lambda f_{PSII} P_S$. Presently we lack detailed mechanistic information about this potential extra source of dNTPs, which would be useful for refining the model. For example, if photosynthesis powers the conversion of a finite cellular resource to dNTPs, the depletion of this resource ought to be modeled.

After accounting for the incorporation of free dNTPs into genomes, we have a rate equation for dNTPs per cell (N):

$$\frac{d(N)}{dt} = s_G + s_P - 2\frac{V_r N}{N + K_{mr}} P_r. \quad (4)$$

We next model the proportion of PSII subunits that are functional (f_{PSII}), to insert in both s_G and s_P. Functional PSII subunits are lost when their D1 proteins become damaged. Following excision of the damaged D1 protein, PSII subunits become functional upon receiving a new D1 protein. Our approach is similar to that of [26], in modeling the proportions of PSII subunits that (i) are functional (f_{PSII}), (ii) contain damaged D1 proteins (d_{PSII}), and (iii) have had damaged D1 proteins excised ('empty' PSII subunits, or x_{PSII}) (Fig. 1). For functional and damaged subunits, we track PSII subunits containing host- versus phage-encoded D1 proteins separately. For example, for functional PSII subunits, $f_{PSII} = f_{PSIIH} + f_{PSIIP}$, where f_{PSIIH} and f_{PSIIP} contain host D1 and phage D1, respectively. We also assume that during the course of infection, the total number of PSII subunits (U) in a cell is constant, and that $f_{PSIIH} + f_{PSIIP} + d_{PSIIH} + d_{PSIIP} + x_{PSII} = 1$. This yields the following system of equations:

$$\frac{d(f_{PSIIH})}{dt} = -k_{D1dam} f_{PSIIH} + k_{\tau D1} R_{HpsbA} x_{PSII} \quad (5)$$

$$\frac{d(d_{PSIIH})}{dt} = k_{D1dam} f_{PSIIH} - k_{exc} d_{PSIIH} \quad (6)$$

$$\frac{d(f_{PSIIP})}{dt} = -k_{D1dam} f_{PSIIP} + k_{\tau D1} R_{PpsbA} x_{PSII} \quad (7)$$

$$\frac{d(d_{PSIIP})}{dt} = k_{D1dam} f_{PSIIP} - k_{exc} d_{PSIIP}, \quad (8)$$

where $x_{PSII} = 1 - (f_{PSIIH} + f_{PSIIP} + d_{PSIIH} + d_{PSIIP})$. Here k_{D1dam} is the rate

at which D1 proteins in functional PSII subunits are damaged by irradiance, k_{exc} is the rate at which damaged D1 proteins are excised from PSII subunits, and $k_{\tau D1}$ is the rate at which damaged PSII subunits are repaired using *psbA* mRNA transcripts. R_{HpsbA} and R_{PpsbA} are the abundances of host and phage *psbA* transcripts, respectively. This formulation assumes that D1 proteins are represented only in functional and damaged PSII subunits, and that *psbA* transcripts are limiting to repair.

The expression of host and phage *psbA* transcripts are modeled as follows:

$$\frac{d(R_{HpsbA})}{dt} = k_{HpsbA} G_H (1 - P_{Rpol}) - d_{RpsbA} R_{HpsbA} \qquad (9)$$

$$\frac{d(R_{PpsbA})}{dt} = k_{PpsbA} P_{PpsbA} - d_{RpsbA} R_{PpsbA}. \qquad (10)$$

Here d_{RpsbA} is the decay rate of *psbA* mRNA transcripts. k_{HpsbA} and k_{PpsbA} are the maximum rates of transcription of host and phage *psbA* mRNAs, respectively. Host *psbA* is transcribed until either the host genome is gone, or until host RNA polymerase is inhibited. The inhibition of host RNA polymerase by a phage protein is represented using the term (1-P_{Rpol}), where P_{Rpol} is a Hill function. P_{PpsbA} is a Hill function representing the commencement of transcription of phage *psbA* at a time of approximately t_{PpsbA}.

The above formulation includes assumptions that can be tested experimentally, and improved in future versions of the model. We assume, for example, that host and phage *psbA* transcripts have identical rates of decay (d_{RpsbA}). We also assume that empty PSII subunits can be repaired at identical rates using products of host and phage *psbA* genes, that PSII subunits containing host and phage D1 proteins have similar rates of damage (k_{D1dam}) and excision (k_{exc}), and that functional PSII subunits containing host and phage D1 have similar rates of photosynthesis. In reality, these properties of host and phage *psbA* transcripts or D1 proteins could be different. For example, it has been suggested that phage D1 might be more resistant to photodamage than host D1 [28]. Furthermore, we assume that the total number of photosystem II subunits and the maximum rates of excision and repair are constant over the course of infection, while in reality, these values may decay as a function of time. It would be useful to measure these properties of infected cells experimentally, and revise the model if necessary. More broadly, our model clearly uses a highly simplified representation of photosynthesis, an extremely complex process influenced by a large number of factors [29]. Our goal was to abstract this complexity with a focus on the potential advantage to phage of supplementing the supply of D1 during infection.

Results

Model validation

(a) Approach. The parameterization of the model is described in detail below, and parameter values are listed in Table 1. Our general approach was as follows: We began by considering parameters that govern the abundance of host and phage *psbA* transcripts, and then estimated parameters for the abundance of host and phage D1 proteins. In the experiments that are the basis for the model, cells were grown under continuous light [17]. We therefore assumed the abundances of host *psbA* mRNAs and the proportions of functional, damaged and empty PSII subunits were in steady state prior to infection, and set equations (5), (6) and (9) equal to 0. This imposed relationships between parameters and initial conditions of some variables (Table 1), reducing the number of free parameters. Finally, we used data for genome replication in the light and dark [17] to estimate parameters for the dependence of dNTP acquisition on photosynthesis. Data from Lindell et al. [20] were used to estimate parameters for the degradation of host genomes and for the timing of expression of phage genes involved in genome replication and dNTP production (see Text S1).

Lindell et al. [17,20] studied populations of cells that were infected with phage, while our model is based on infection of a single host cell. In comparing model predictions to these experimental data, we assume that our model represents infection of an average cell. To estimate the number of phage genomes per host cell at different times after infection, we normalized by the number of phages measured at 1 h post-infection. Given that our estimates of phage genome replication depend on this normalization, we place our emphasis on the proportional advantage or disadvantage conferred by phage *psbA*, rather than the absolute number of genomes. Lindell et al. [17] used a low multiplicity of infection (0.1 phage for every host cell) for the experiment in which phage genome replication was measured. Under these conditions, most infected cells would have been infected by a single virion. When using data for intracellular levels of host *psbA* transcripts, D1 proteins, and genomes, we assumed that 50% of cells were infected (see Text S1 for analyses that consider the implications of varying this assumption). A higher multiplicity of infection (3 phage per host cell) was used in the experiments from which these data were collected, and 50% represents the maximum level of infection that has been observed for this phage [17]. We also assumed that measurements of D1 protein abundance made by [17] detected both functional and damaged D1 proteins.

We integrated equations (1)–(10) using ode45, a MATLAB® (The MathWorks, Natick, MA) variable time step numerical ODE solver, which implements a medium order Runge-Kutta scheme.

(b) Expression of photosynthesis genes. Experimental evidence shows that following infection by the cyanophage P-SSP7, the abundance of *psbA* transcripts in the host cell declines [17]. We assumed that host transcription was largely inhibited (1-$P_{Rpol} \approx 0$) by 1 hour after infection (Fig. 2A, Table 1), and calculated the decay constant (d_{RpsbA}) using experimental observations [17]. We set the initial value of host *psbA* mRNA to $R_{HpsbA}(0) = 1$, and normalized the abundance of host *psbA* transcripts to this initial (maximum) value.

Following the decay of host *psbA* transcripts, Lindell et al. [17] observed a drop in the level of host D1 proteins, such that host D1 abundance had decreased to approximately 45% of its maximum value (measured 1 hour after infection) after 8 hours of infection (Fig. 2B). In parameterizing the dynamics of host D1 proteins, we first assumed cells were in steady state prior to infection, which constrained parameters according to $R_{HpsbA}(0)k_{\tau D1}x_{PSII}(0) = k_{exc}d_{PSIIH}(0) = k_{D1dam}f_{PSIIH}(0)$. This means only $x_{PSII}(0)$ (and correspondingly, $k_{\tau D1}$; see Table 1) was free to vary for given pair of k_{exc} and k_{D1dam} values (since $R_{HpsbA}(0) = 1$, and $x_{PSII}(0) + d_{PSIIH}(0) + f_{PSIIH}(0) = 1$). We did not have independent estimates of the parameters k_{D1dam}, k_{exc} and $x_{PSII}(0)$ for *Prochlorococcus* under the conditions of the experiment [17], and values of k_{D1dam} and k_{exc} may vary substantially among organisms and growth conditions [26]. We therefore used measurements from a study of *Prochlorococcus* PSII function and D1 protein abundance under transient exposure to high irradiance [30] to estimate possible ranges of parameters k_{D1dam}, k_{exc} and $x_{PSII}(0)$. We then solved our model of D1 dynamics 3060 times, comprising all combinations of 17 values of k_{D1dam}, 15 values of k_{exc}, and 12 values of $x_{PSII}(0)$ (see Table 1). Out of these 3060 simulations, 126 resulted in a drop in

Table 1. Model parameters and initial conditions.

Parameter	Description	Units	Value
G_P	phage genomes	genomes cell^{-1}	1*
G_H	host genomes	genomes cell^{-1}	1*
G_{Hdeg}	degraded host genomes	genomes cell^{-1}	0
N	dNTPs	dNTPs cell^{-1}	0
f_{PSIIH}, f_{PSIIP}	proportion of PSII subunits that are functional and contain host, phage D1	dimensionless	$\frac{1-x_{PSII}}{1+\frac{k_{D1dam}}{k_{exc}}}=0.46$, 0*
d_{PSIIH}, d_{PSIIP}	proportion of PSII subunits that are damaged and contain host, phage D1	dimensionless	$\frac{1-x_{PSII}}{1+\frac{k_{exc}}{k_{D1dam}}}=0.04$, 0*
x_{PSII}	proportion of PSII subunits that are empty	dimensionless	0.5*,[a]
R_{HpsbA}, R_{PpsbA}	*psbA* transcripts	dimensionless	1, 0*
L_H, L_P	genome length of host, phage	bp genome^{-1}	1657990, 44970
V_r	max velocity of phage DNA elongation	bp h^{-1} cell^{-1}	1332000
K_{mr}	half-saturation for DNA replication	dNTP cell^{-1}	1224
t_r	timing parameter for phage genome replication	h	2
V_{Gdeg}	max velocity of host genome degradation	genomes cell^{-1} h^{-1}	0.35
K_{mGH}	half-saturation for host genome degradation	genomes cell^{-1}	0.000001
t_{Gdeg}	timing parameter for host genome degradation	h	5
ε	production of dNTPs from degraded host genome in the dark	dNTP h^{-1} cell^{-1}	127665
κ	production of dNTPs from degraded host genome in the light	dNTP h^{-1} cell^{-1}	0
K_N	half saturation for dNTP production from degraded host genome	genomes cell^{-1}	0.000001
λ	production of dNTPs in the light	dNTP h^{-1} cell^{-1}	1027800
t_S	timing of dNTP synthesis from source s_P	h	4
k_{D1dam}	damage to functional D1 proteins	h^{-1}	0.35[a]
k_{exc}	excision of damaged D1 proteins	h^{-1}	4[a]
$k_{\tau D1}$	repair of empty PSII subunits	h^{-1}	$\frac{k_{exc}d_{PSIIH}}{R_{HpbsA}x_{PSII}}=0.32$
d_{RpsbA}	*psbA* transcript decay	h^{-1}	0.27[b]
k_{HpsbA}	host *psbA* transcription	h^{-1} (genomes cell^{-1})$^{-1}$	0.27[b]
k_{PpsbA}	phage *psbA* transcription	h^{-1}	0.016
t_{Rpol}	timing parameter for inhibition of host RNA polymerase	h	1
t_{PpsbA}	timing parameter for transcription of phage *psbA*	h	1.3
n	Hill parameter	dimensionless	5

*Initial condition.

[a]Values were systematically varied in exploring the kinetics of D1 protein degradation, excision and repair. All combinations of the following values were used:
k_{D1dam} = [0.01, 0.025, 0.05, 0.06, 0.07, 0.08, 0.09, 0.1, 0.125, 0.15, 0.175, 0.2, 0.25, 0.3, 0.35, 0.4, 0.5].
k_{exc} = [0.5, 0.75, 1, 1.25, 1.5, 1.75, 2, 2.5, 3, 3.5, 4, 4.5, 5, 7.5, 10].
$x_{PSII}(0)$ = [0.05, 0.1, 0.15, 0.2, 0.25, 0.3, 0.4, 0.5, 0.6, 0.7, 0.8, 0.9].

[b]This estimate is based on microarray measurements of host *psbA* mRNA expression. Measurements of host *psbA* transcript abundances that were made using RT-PCR [17] suggested a greater value of d_{RpsbA}. We therefore present additional analyses based on a value of $d_{RpsbA}=0.72$ in Text S1.

doi:10.1371/journal.pone.0003550.t001

the abundance of host D1 proteins after 8 hours of infection that was similar to the value measured in the laboratory [17]. From here onward, we present analyses that focus on one set of parameters ($k_{D1dam}=0.35$ and $k_{exc}=4$, with $x_{PSII}(0)=0.5$), but we did perform all subsequent analyses using all 126 combinations of parameters, to confirm that our conclusions are robust across this range of parameter values (see Text S1). The model can provide a reasonable description of the drop in host D1 proteins during infection, as illustrated in Fig. 2B (black line and symbols). However, we note that the model does not predict several features of the experimental observations, and in particular, the low level of host D1 at 0 hours, and the sudden drop in host D1 between 4 hours and 5 hours after infection. We are not aware of any mechanisms that might account for these observations, so have not attempted to replicate them with the present model.

We next modeled the abundance of phage *psbA* transcripts using the decay constant (d_{RpsbA}) calculated above for host *psbA* transcripts. Our model describes the shape of the experimentally derived curve of phage *psbA* mRNA abundance reasonably well (Fig. 2A), though modeled levels of mRNAs approached an asymptotic level more slowly than observed [17].

The empirical observation that phage D1 proteins accumulated to approximately 10% of all D1 after 8 hours of infection [17] was predicted by the model when phage *psbA* transcription was set to 5.9% of the rate at which host *psbA* was transcribed prior to infection ($k_{PpsbA}=0.016$; Fig. 2B), and with the same values of k_{D1dam} and k_{exc} that were used for host D1. The model predicted the increase in the level of phage D1 slightly sooner than it was observed experimentally. This could be due to a time delay for the translation of D1, or may simply reflect experimental variability.

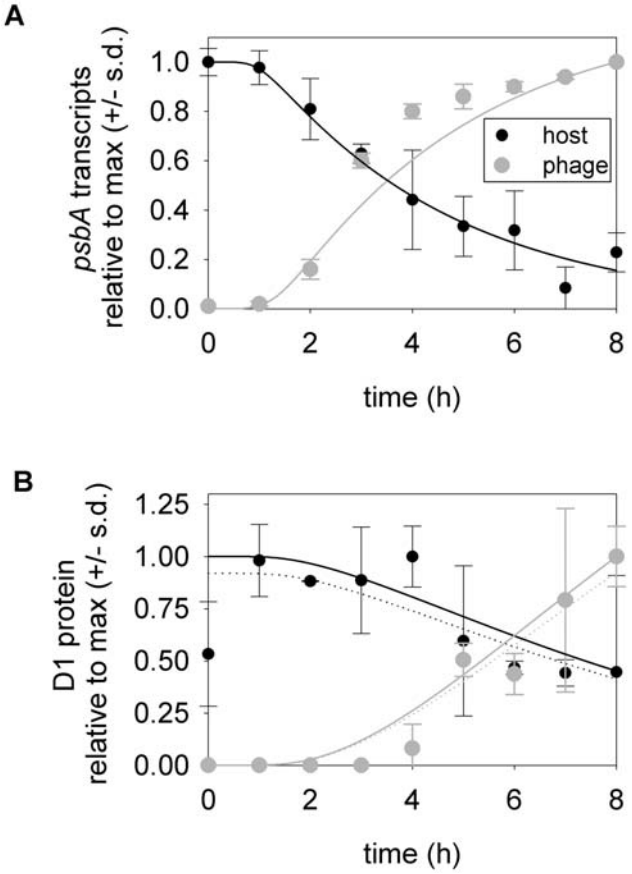

Figure 2. Measured (data points) and modeled (lines) levels of host and phage *psbA* transcripts (A) and D1 protein product (B) during the lytic cycle of infection of *Prochlorococcus* MED4 by cyanophage P-SSP7. For modeled levels of D1 protein, solid lines represent the sum of functional and damaged D1, and dotted lines represent functional D1 only. Data are from [17]. Data for host expression levels were transformed assuming that 50% of cells were infected [17].
doi:10.1371/journal.pone.0003550.g002

(**c**) **Degradation of the host genome.** Experimental evidence showed that host genomes are mostly degraded between 4 and 8 hours after infection [20] and the loss of host genomes was approximately linear. The model provides a good description of these observations with $t_{Gdeg} = 5$ and $V_{Gdeg} = 0.35$, and with K_{mGH} set to a small value (0.000001) (data not shown).

(**d**) **Genome replication.** To study phage genome replication in the model, we first simulate infection in the dark, setting the photosynthesis-dependent production of dNTPs equal to zero (setting $\lambda = 0$ and $\kappa = 0$). We then needed to estimate values for DNA replication kinetic parameters (V_r and K_{mr}), the timing of phage DNA replication machinery (t_r) and the production of dNTPs using degraded host genomes in the absence of photosynthesis (ε). Phage T7 has a rate of DNA elongation of approximately 1,332,000 (h^{-1} polymerase^{-1}) [21,31]. In the absence of data for cyanophage P-SSP7, we set $V_r = 1{,}332{,}000$ (bp h^{-1} $cell^{-1}$). We did not multiply this value by the number of phage polymerases in the host cells since (i) we do not have data on phage polymerase abundance, and (ii) this value of V_r is already sufficiently large to be non-limiting to genome replication (see below). We also estimated K_{mr} based on the corresponding value for deoxynucleotide incorporation by T7 phage enzymes [21,32], adjusted according to the size of a *Prochlorococcus* MED4 cell, which is assumed to be a sphere with diameter 0.6 μm. We assumed that phage genome replication enzymes were expressed approximately 2 hours post-infection ($t_r = 2$), based on observations of phage DNA polymerase transcript abundance in [20] (see Text S1). We then found that $\varepsilon = 127{,}665$ could provide a reasonable description of genome replication in the dark, if all dNTPs used in phage genome replication in the dark were derived from the host genome (Fig. 3).

Our model includes the possibility that photosynthesis increases the production of dNTPs from degraded host genomes, and the possibility that photosynthesis promotes the synthesis of new deoxynucleotides. However, since we do not know the relative importance of these possible sources of dNTPs, we analyze their potential contribution to dNTP production during infection in the light separately. Here we present analyses that assume extra dNTPs made in the light were derived from the synthesis of new deoxynucleotides (i.e., $\lambda > 0$ and $\mu = 0$). However, we confirmed that similar results are obtained if we assume instead that the extra dNTPs made in the light were derived from the degraded host genome (see Text S1).

For infection in the light, we use the same values of parameters V_r, K_{mr}, t_r and ε, and found that $\lambda = 1{,}027{,}800$ (dNTP h^{-1} $cell^{-1}$) gave a reasonable description of phage genome replication (Fig. 3). With this parameterization, dNTP availability is strongly limiting to genome replication: a 10% increase in dNTP production by photosynthesis (λ) results in a 7.3% increase in genome replication, whereas a 10% increase in the maximum velocity of genome replication (V_r) results in almost no increase in genome replication.

In silico knockout of phage *psbA*

The major goal of this study is to consider the fitness consequences to a phage of encoding and expressing the *psbA* gene. Having described the kinetics of infection reasonably well with our model (Figs 2 and 3), we can now turn off transcription of phage *psbA* ($k_{PpsbA} = 0$), and study how this affects the predicted number of phage genomes in infected cells after 8 h of infection. Using the parameter values presented in Table 1, we predict that a phage unable to express *psbA* would produce 2.81% fewer genomes after 8 h of infection. However, if a phage did not encode *psbA*, its genome would be shorter, by approximately

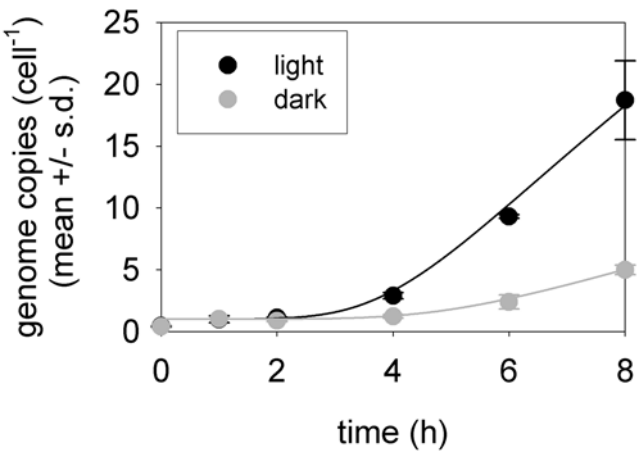

Figure 3. Measured (data points) and modeled (lines) genome copies of cyanophage P-SSP7 during the lytic cycle under light (25 μE m^{-2} s^{-1}) and dark conditions. Genome copies were measured as genomes per ml of culture [17], and were transformed to a per cell basis for comparison to the model.
doi:10.1371/journal.pone.0003550.g003

1080 bp. Taking this into account, a phage that did not encode *psbA* would produce only 0.55% fewer genomes after 8 h of infection than a phage that encodes and expresses *psbA*. In the dark, where there is presumably no advantage to expressing *psbA*, a phage without this gene is predicted to produce 1.97% more genomes than a phage with it.

Ideally, we would like to consider the consequences of *psbA* to phage genome replication under different and changing levels of irradiance. However, many of the parameters used in our model are likely to change as a function of irradiance, in ways that can be difficult to predict (see [29]). Therefore we limit ourselves to one specific case, where cells are moved from 25 μE m^{-2} s^{-1} to 50 μE m^{-2} s^{-1} one hour after infection has begun, when the capacity of the cells to respond to the changing light may be largely compromised by infection. This means we can use the same initial conditions and parameter values as in our previous simulations (Table 1), except for two parameters that will be affected directly by the increased irradiance (k_{D1dam} and λ). We assume that the rate of damage to functional PSII subunits (k_{D1dam}) increases proportionally with irradiance (i.e., k_{D1dam} is doubled; [26]), and that the rate of photosynthesis of *Prochlorococcus* MED4 is greater at 50 μE m^{-2} s^{-1} than at 25 μE m^{-2} s^{-1} by a factor of approximately 1.75 [33,34].

We found that in the case where irradiance increases from 25 μE m^{-2} s^{-1} to 50 μE m^{-2} s^{-1} one hour after infection, a phage that does not express *psbA* is predicted to produce 4.31% fewer genomes than a phage that does. Here, a phage that does not express or encode *psbA* is predicted to produce 2.10% fewer genomes than a phage that does encode and express *psbA*. We therefore predict that *psbA* will have a greater impact on phage genome replication under this switch to a higher level of irradiance, such as could occur in the surface mixed layer of the oceans. We note that this prediction also holds if photosynthesis (and λ) increases by a factor of either 1.5 or 2 under the switch to higher irradiance, rather than by a factor of 1.75 (see Text S1). Further, we performed analyses similar to the above using a range of different values of k_{D1dam}, k_{exc} and $x_{PSII}(0)$. Across these simulations, expressing *psbA* usually led to a modest increase in genome replication in continuous light (of between 2.5 and 4.5%), though this increase was typically smaller (between 0.3 and 2.3%) when the cost of encoding *psbA* was considered. The predicted advantage of expressing and encoding *psbA* was typically greater when a switch to higher light was simulated during infection, though the precise size of the advantage conferred by *psbA* varied (see Text S1).

Cyanophage dNTP diets

In addition to *psbA*, marine cyanophages encode a variety of genes that potentially help them acquire dNTPs (*e.g.*, ribonucleotide reductase, transaldolase; see [35]). It is therefore interesting to ask more broadly: Under what set of circumstances can a phage increase its total genome replication by encoding an additional gene or module of genes that help it acquire extra dNTPs?

Consider a phage that encodes genes that allow it to access dNTPs from a single source, s_1 (*e.g.* scavenging from the host genome). Now, a mutant acquires an extra gene or module of genes that allow it to access an extra source of dNTPs, s_2. If genes needed to access this second source of dNTPs elongate the wild type genome, we want to know when the mutant will make more genomes than the wild type by some time post-infection, or when

$$G_M(t) > G_W(t), \tag{10}$$

where $G_M(t)$ and $G_W(t)$ are the numbers of genomes in cells infected by mutant and wild type phages (respectively) at time t.

We explore this question using our original model as a starting point, but with modifications that allow it to be studied analytically. We assume that the supply of dNTPs is highly limiting to genome replication ($N \ll K_{mr}$), such that we can rewrite equation (1) as $\frac{d(G_P)}{dt} \approx \frac{1}{L_P} V_R N$, where V_R is the rate of DNA elongation (here in bp $dNTP^{-1}$ h^{-1} $cell^{-1}$). We also assume that the dNTP revenue from each phage-encoded source can be expressed as a function of time, such that a phage using s_1 and s_2 has $\frac{d(N)}{dt} = s_1(t) + s_2(t) - 2V_R N$. In reality, processes of phage-encoded dNTP acquisition (s_1 and s_2) and genome replication may begin at different times post-infection. For simplicity, we assume these processes all begin at the same time (t_b hours after infection), and let time $t = 0$ in this model refer to this time t_b when these processes begin. Solving for $N(t)$, and then $G_P(t)$ yields

$$G_P(t) = 1 + \frac{1}{2L_P}[N_b(1-\exp(-2V_R t)) + s_1(t) * (1-\exp(-2V_R t)) + s_2(t) * (1-\exp(-2V_R t))] \tag{11}$$

where N_b is the number of dNTPs in the cell at time t_b, there is one phage genome in the cell at time t_b, and '*' represents a convolution product. If we assume N_b is very small ($N_b \approx 0$) and sub (11) into (10), we get

$$\frac{1}{2(L_R + L_1 + L_2)}[\Psi_1 + \Psi_2] > \frac{1}{2(L_R + L_1)}[\Psi_1], \tag{12}$$

where Ψ_1 and Ψ_2 represent dNTPs derived from s_1 and s_2 (respectively), L_1 and L_2 represent the length of genes needed to encode s_1 and s_2 (respectively) and L_R represents the length of the rest of the genome. This can be expressed as $\frac{\Psi_2}{\Psi_1} > \frac{L_2}{(L_R + L_1)}$, meaning that a new module of genes will increase phage genome replication if it leads to a proportional increase in dNTP production that is greater than the proportional increase in genome length that it causes. Alternatively, we could say that for a new module of genes to increase phage genome replication, it must have a ratio of dNTPs contributed / cost in genome length, $\frac{\Psi_2}{L_2}$, that exceeds a threshold, $\frac{\Psi_1}{(L_R + L_1)}$.

While this model is oversimplified, and has required assumptions that limit its applicability, it nevertheless may help us to understand some of the variability among cyanophages in methods they use to acquire dNTPs. For example, it suggests that if two similar phages acquire dNTPs by scavenging from the genomes of their hosts (i.e., their s_1), but one phage infects a host with a smaller genome from which fewer dNTPs can be produced (smaller Ψ_1), this phage might be more likely to exploit an additional source of dNTPs, if given the opportunity. This may be one factor that helps to explain why cyanophages infecting *Prochlorococcus*, which has a very small genome, might encode genes that help acquire dNTPs from other sources (see [36] for discussion of related issues).

Further, it can be shown that if the new source of dNTPs, s_2, is highly profitable, the phage may no longer be advantaged by encoding s_1. We would expect this to be the case when $\frac{1}{2(L_R + L_2)}[\Psi_2] > \frac{1}{2(L_R + L_1 + L_2)}[\Psi_1 + \Psi_2]$, or when $\frac{\Psi_2}{(L_R + L_2)} > \frac{\Psi_1}{L_1}$. This illustrates a way in which one source of dNTPs could replace another in the genome of a phage, over evolutionary time.

This analysis has strong parallels with diet theory models that predict when a foraging animal should incorporate an encountered prey item into its diet, based on the energetic gain from the prey item, balanced against the cost in terms of time of pursuing it [37,38]. It thus adds to an impressive list of circumstances in which

phage strategies can be understood using analogies to theory developed for foraging animals (*e.g.* [39,40]).

Discussion

The goal of this simple modeling exercise was to predict the advantage conferred to a cyanophage of carrying and expressing the *psbA* gene. More specifically, we consider the hypothesis that phage *psbA* expression augments the photosynthetic apparatus of the host during infection, following the decay of host *psbA* transcripts, and we do not consider possible alternative or additional advantages of phage *psbA*. We have intentionally oversimplified the complex processes of infection, photosynthesis and dNTP synthesis in an effort to match the model to the scope and resolution of the available data. The modeled predictions serve as hypotheses to be tested when the means to knock out specific genes in these cyanophage genomes are eventually developed.

First, we predict that under low continuous irradiance, phage *psbA* expression increases phage genome replication, and potentially phage fitness, relative to a 'mutant' that does not contain this gene. This advantage is substantially reduced, however, if one accounts for the cost to the phage of elongation of the cyanophage P-SSP7 genome by *psbA*. Second, we predict that the slight advantage conferred by phage-encoded *psbA* may be greater under conditions of light stress, such as an increase in irradiance during infection. This is due to the more rapid decay of host D1 proteins at higher irradiance, and could contribute substantially to the advantage conferred by *psbA* to cyanophage P-SSP7 in the dominant habitat of this particular *Prochlorococcus* host — the surface mixed layer of the ocean. Finally, the model predicts that during infection in the dark, where there is presumably no advantage to expressing *psbA*, encoding *psbA* would result in a net decrease in genome replication of approximately 2%. Taken together, these results illustrate how the benefits of *psbA* to cyanophage genome replication may vary substantially among infections that occur at different times over the diel cycle, or for cells that are subject to different conditions of irradiance due to mixing [18]. These are all testable hypotheses.

It is clear that the selective advantage of *psbA* to phage will be determined by the benefit it confers during all conditions under which infection occurs, weighted by their frequency of occurrence. Therefore to fully understand the fitness consequences of carrying the *psbA* gene to phage, we will need to better understand how *psbA* influences genome replication over a much broader range of conditions, including at different times over the diel cycle where properties of host photosynthesis will change dynamically [29] and hosts will contain different numbers of genomes [41] and free dNTPs. To connect these predictions for genome replication to fitness, we will also need a better understanding of when genome replication limits phage burst size (*e.g.* see [24,42,43]) and of the interactions between burst size and other factors, such as the timing of cell lysis, and the availability and quality of hosts (*e.g.* [39,40,44–47]).

We have learned recently that marine cyanophage encode a number of genes that are absent in the genomes of non-marine phages and share homology with genes involved in microbial metabolism [11]. As we attempt to understand both the evolutionary significance of these genes and the distribution of phage genes in the ocean [35], it will be useful to have theoretical tools. To begin building such tools, here we have developed a model exploring the selective advantage of one specific gene of host origin that is commonly encoded by marine cyanophages, as well as more general tradeoffs between acquiring dNTPs and elongating the genome. We hope these models will form the basis for a more powerful and predictive modeling framework, and contribute substantially to our understanding of phage dynamics in marine microbial communities.

Supporting Information

Text S1 Description of simulations using a range of different parameter values.
Found at: doi:10.1371/journal.pone.0003550.s001 (0.34 MB PDF)

Acknowledgments

We thank S. Abedon, D. Campbell, D. Lindell, M. Follows and S. Dutkiewicz for valuable comments on earlier versions of this manuscript. We thank M. Sullivan, D. Lindell, D. Endy and members of the Chisholm lab for helpful discussions of this work.

Author Contributions

Conceived and designed the experiments: JGB. Analyzed the data: JGB. Wrote the paper: JGB SWC.

References

1. Partensky F, Hess WR, Vaulot D (1999) *Prochlorococcus*, a marine photosynthetic prokaryote of global significance. Microbiology and Molecular Biology Reviews 63: 106–127.
2. Bouman HA, Ulloa O, Scanlan DJ, Zwirglmaier K, Li WKW, et al. (2006) Oceanographic basis of the global surface distribution of *Prochlorococcus* ecotypes. Science 312: 918–921.
3. Johnson ZI, Zinser ER, Coe A, McNulty NP, Woodward EMS, et al. (2006) Niche partitioning among *Prochlorococcus* ecotypes along ocean-scale environmental gradients. Science 311: 1737–1740.
4. Mann NH (2003) Phages of the marine cyanobacterial picophytoplankton. FEMS Microbiology Reviews 27: 17–34.
5. Waterbury JB, Valois FW (1993) Resistance to co-occurring phages enables marine *Synechococcus* communities to coexist with cyanophages abundant in seawater. Applied and Environmental Microbiology 59: 3393–3399.
6. Suttle CA, Chan AM (1994) Dynamics and distribution of cyanophages and their effect on marine *Synechococcus* spp. Applied and Environmental Microbiology 60: 3167–3174.
7. Sullivan MB, Waterbury JB, Chisholm SW (2003) Cyanophages infecting the oceanic cyanobacterium *Prochlorococcus*. Nature 424: 1047–1051.
8. DeLong EF, Preston CM, Mincer T, Rich V, Hallam SJ, et al. (2006) Community genomics among stratified microbial assemblages in the ocean's interior. Science 311: 496–503.
9. Chen F, Lu J (2002) Genomic sequence and evolution of marine cyanophage P60: a new insight on lytic and lysogenic phages. Applied and Environmental Microbiology 68: 2589–2594.
10. Mann NH, Clokie MRJ, Millard A, Cook A, Wilson WH, et al. (2005) The genome of S-PM2, a "photosynthetic" T4-type bacteriophage that infects marine *Synechococcus* strains. Journal of Bacteriology 187: 3188–3200.
11. Sullivan MB, Coleman ML, Weigele PR, Rohwer F, Chisholm SW (2005) Three *Prochlorococcus* cyanophage genomes: signature features and ecological interpretations. PloS Biology 3: e144.
12. Mann NH, Cook A, Millard A, Bailey S, Clokie M (2003) Marine ecosystems: bacterial photosynthesis genes in a virus. Nature 424: 741–741.
13. Lindell D, Sullivan MB, Johnson ZI, Tolonen AC, Rohwer F, et al. (2004) Transfer of photosynthesis genes to and from *Prochlorococcus* viruses. Proceedings of the National Academy of Sciences of the United States of America 101: 11013–11018.
14. Millard A, Clokie MRJ, Shub DA, Mann NH (2004) Genetic organization of the *psbAD* region in phages infecting marine *Synechococcus* strains. Proceedings of the National Academy of Sciences of the United States of America 101: 11007–11012.
15. Sullivan MB, Lindell D, Lee JA, Thompson LR, Bielawski JP, et al. (2006) Prevalence and evolution of core photosystem II genes in marine cyanobacterial viruses and their hosts. PLoS Biology 4: 1344–1357.
16. Ohad I, Kyle DJ, Arntzen CJ (1984) Membrane protein damage and repair: removal and replacement of inactivated 32-kilodalton polypeptides in chloroplast membranes. Journal of Cell Biology 99: 481–485.
17. Lindell D, Jaffe JD, Johnson ZI, Church GM, Chisholm SW (2005) Photosynthesis genes in marine viruses yield proteins during host infection. Nature 438: 86–89.

18. Bailey S, Clokie MRJ, Millard A, Mann NH (2004) Cyanophage infection and photoinhibition in marine cyanobacteria. Research in Microbiology 155: 720–725.
19. Mackenzie JJ, Haselkorn R (1972) Photosynthesis and the development of blue-green algal virus SM-1. Virology 49: 517–521.
20. Lindell D, Jaffe JD, Coleman ML, Futschik ME, Axmann IM, et al. (2007) Genome-wide expression dynamics of a marine virus and its host reveal features of co-evolution. Nature 449: 83–86.
21. Endy D, Kong D, Yin J (1997) Intracellular kinetics of a growing virus: a genetically structured simulation for bacteriophage T7. Biotechnology and Bioengineering 55: 375–389.
22. Endy D, You L, Yin J, Molineux IJ (2000) Computation, prediction, and experimental tests of fitness for bacteriophage T7 mutants with permuted genomes. Proceedings of the National Academy of Sciences of the United States of America 97: 5375–5380.
23. You L, Yin J (2002) Dependence of epistasis on environment and mutation severity as revealed by *in silico* mutagenesis of phage T7. Genetics 160: 1273–1281.
24. You L, Suthers PF, Yin J (2002) Effects of *Escherichia coli* physiology on growth of phage T7 *in vivo* and *in silico*. Journal of Bacteriology 184: 1888–1894.
25. Buchholtz F, Schneider FW (1987) Computer simulation of T3 / T7 phage infection using lag times. Biophysical Chemistry 26: 171–179.
26. Tyystjärvi E, Mäenpää P, Aro E-M (1994) Mathematical modelling of photoinhibition and Photosystem II repair cycle. I. Photoinhibition and D1 protein degradation in vitro and in the absence of chloroplast protein synthesis in vivo. Photosynthesis Research 41: 439–449.
27. Murray JD (1989) Mathematical biology. Berlin: Springer-Verlag.
28. Sharon I, Tzahor S, Williamson S, Shmoish M, Man-Aharonovich D, et al. (2007) Viral photosynthetic reaction center genes and transcripts in the marine environment. ISME Journal 1: 492–501.
29. Falkowski PG, Raven JA (2007) Aquatic photosynthesis. Princeton, NJ: Princeton University Press.
30. Six C, Finkel ZV, Irwin AJ, Campbell DA (2008) Light variability illuminates niche-partitioning among marine picocyanobacteria. PLoS One 2: e1341.
31. Rabkin SD, Richardson CC (1990) *In vivo* analysis of the initiation of bacteriophage T7 DNA replication. Virology 174: 585–592.
32. Donlin MJ, Johnson KA (1994) Mutants affecting nucleotide recognition by T7 DNA polymerase. Biochemistry 33: 14908–14917.
33. Moore LR, Chisholm SW (1999) Photophysiology of the marine cyanobacterium *Prochlorococcus*: ecotypic differences among cultured isolates. Limnology and Oceanography 44: 628–638.
34. Partensky F, Hoepffner N, Li WKW, Ulloa O, Vaulot D (1993) Photoacclimation of *Prochlorococcus* sp. (Prochlorophyta) strains isolated from the north Atlantic and the Mediterranean sea. Plant Physiology 101: 285–296.
35. Breibart M, Thompson LR, Suttle CA, Sullivan MB (2007) Exploring the vast diversity of marine viruses. Oceanography 20: 135–139.
36. Brown CM, Lawrence JE, Campbell DA (2006) Are phytoplankton population density maxima predictable through analysis of host and viral genomic DNA content? Journal of the Marine Biological Association of the United Kingdom 86: 491–498.
37. MacArthur RH, Pianka ER (1966) On optimal use of a patchy environment. American Naturalist 100: 603–609.
38. Schoener TW (1971) Theory of feeding strategies. Annual Review of Ecology and Systematics 2: 369–404.
39. Wang I-N, Dykhuizen DE, Slobodkin LB (1996) The evolution of phage lysis timing. Evolutionary Ecology 10: 545–558.
40. Bull JJ (2006) Optimality models of phage life history and parallels in disease evolution. Journal of Theoretical Biology 241: 928–938.
41. Vaulot D, Marie D, Olson RJ, Chisholm SW (1995) Growth of *Prochlorococcus*, a photosynthetic prokaryote, in the equatorial pacific ocean. Science 268: 1480–1482.
42. Kim H, Yin J (2004) Energy-efficient growth of phage Q beta in *Escherichia coli*. Biotechnology and Bioengineering 88: 148–156.
43. You L, Yin J (2006) Evolutionary design on a budget: robustness and optimality of bacteriophage T7. IEE Proceedings Systems Biology 153: 46–52.
44. Abedon ST (1989) Selection for bacteriophage latent period length by bacterial density: a theoretical examination. Microbial Ecology 18: 79–88.
45. Abedon ST, Herschler TD, Stopar D (2001) Bacteriophage latent period evolution as a response to resource availability. Applied and Environmental Microbiology 67: 4233–4241.
46. Abedon ST, Hyman P, Thomas C (2003) Bacteriophage latent-period evolution as a response to bacteria availability: An experimental examination. Applied and Environmental Microbiology 69: 7499–7506.
47. Wang I-N (2006) Lysis timing and bacteriophage fitness. Genetics 172: 17–26.